Opto-Electronic Advances

Supplementary information

2022, Vol. 5, No. 11

DOI: 10.29026/oea.2022.210047

Spatiotemporal Fourier transform with femtosecond pulses for on-chip devices

Yulong Wang[1,2], Changjun Min[1]*, Yuquan Zhang[1] and Xiaocong Yuan[1]*

[1]Nanophotonics Research Centre, Shenzhen Key Laboratory of Micro-Scale Optical Information Technology & Institute of Microscale Optoelectronics, Shenzhen University, Shenzhen 518060, China; [2]Songshan Lake Materials Laboratory, Dongguan 523808, China.
*Correspondence: CJ Min, E-mail: cjmin@szu.edu.cn; XC Yuan, E-mail: xcyuan@szu.edu.cn

This file includes:

Supplementary information for this paper is available at https://doi.org/10.29026/oea.2022.210047

Section 1: The dependence of the spatiotemporal FT effects on the radius *R* in the case of angular dispersion (θ =10°).

Figure S1 shows the influence of *R* on the space-time focusing properties of the SPP pulse. When the radius is small (*R* =10 μm), the SPP pulse converges along the upper right direction (*t* =–6.7 fs) before diverges along the lower right direction (*t* =6.7 fs), and forms a slightly tilted focus at *t* =0 fs (Fig. S1(a)). Due to the relatively small radius, the excited SPP pulse has a short propagation distance, making the accumulated dispersion effect very small, resulting in the insignificant spatiotemporal differences of different frequency components in the focal plane. Therefore, when the radius increases (*R* =25 μm), the wavefront of the SPP pulse appears as a curved arc at different times, and the direction of its bending greatly rotates with time (Fig. S1(b)), and forming an inverted C shape at *t* =0 fs. When the radius is further increased, such as *R*=40 μm, sufficient dispersion effects are accumulated during the propagation of the SPP pulse, so that the instantaneous wavefront is bent into a ring (Fig. 2(l)). Meaning that the propagation path of the SPP pulse can be effectively modulated by changing the radius of the arc.

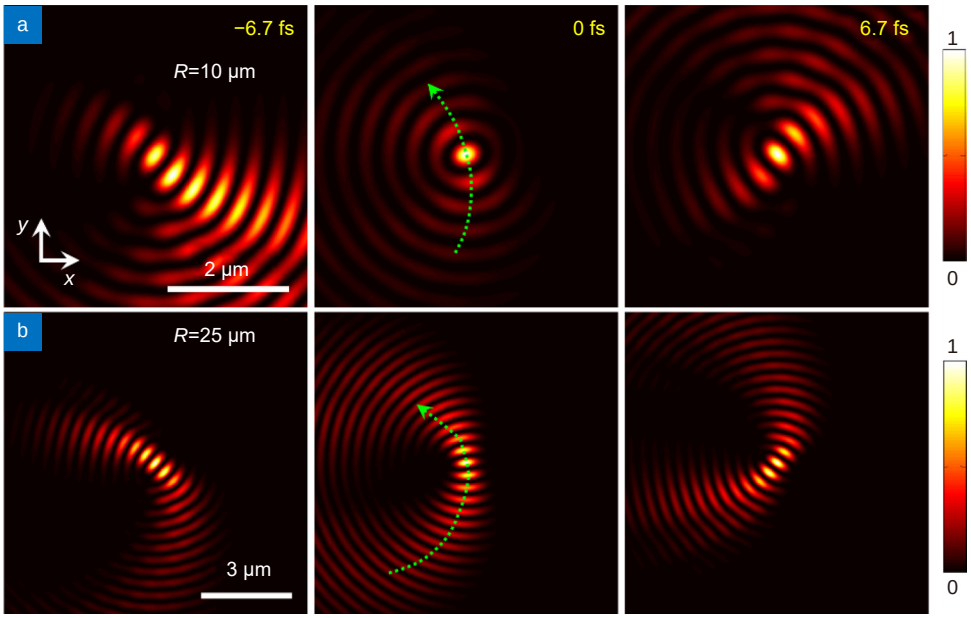

Fig. S1 | The dependence of the spatiotemporal FT effects on the radius *R* in the case of angular dispersion (θ =10°). (**a**) *R* =10 μm, α =180°, τ =10 fs. (**b**) The same as (a) except *R* =25 μm. The green arrow indicates the direction of propagation path of the SPP pulses at the elapsed time given in the top right corner.

Section 2: The dependence of the spatiotemporal FT effects on the arc measure α in the case of angular dispersion (θ =10°).

Figure S2 shows the influence of α on the space-time focusing properties of the SPP pulse. The wavefront of the SPP pulse always remains bend to the left with time, except for the changes in the height of the head and tail (Fig. S2). Compared with Fig. 2(l), it can be found that as α decreases, the spatiotemporal curvature of the SPP pulse in the focal region decreases accordingly, especially at *t*=0 fs, the SPP pulse degenerates from a ring to inverted C shape. This is because the tightly focused SPP pulse gradually becomes weakly focused as α decreases, leading to the increase of focal depth. Proving that the arc measure may has a great influence on the spatiotemporal FT effect of the SPP pulse.

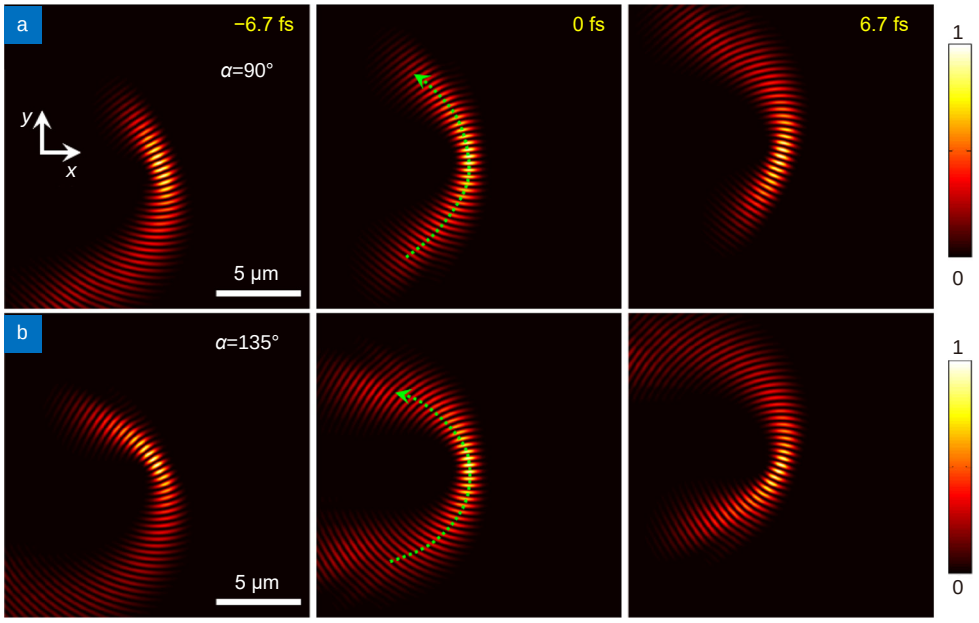

Fig. S2 | The dependence of the spatiotemporal FT effects on the arc measure α in the case of angular dispersion (θ =10°). (**a**) R =40 μm, α =90°, τ =10 fs. (**b**) The same as (a) except α =135°. The green arrow indicates the direction of propagation path of the SPP pulses at the elapsed time given in the top right corner.

Section 3: The dependence of the spatiotemporal FT effects on the pulse durations τ in the case of angular dispersion (θ =10°).

We also further analyzed the ultrafast spatiotemporal FT process of SPP pulses excited by light sources with different pulse durations τ (Fig. S3). The SPP pulse excited by a light source with a shorter pulse duration (τ =5 fs) shows a spiral shape (t =−3.4 fs), and then forms a ring at t =0 fs (Fig. S3(a)), and further evolves into another spiral with opposite rotation directions (t =3.4 fs). However, when excited by a longer pulse (τ =20 fs), the instantaneous ring-shape disappears, except a slightly bended propagation path (Fig. S3(b)). Compared with Fig. 2(l), we found that the shorter the pulse duration, the more severely the propagation path is bent. Because, the excitation light source has more sufficient frequency components, which equivalently amplifies the dispersion effect of the SPP pulses. Proving that the spatiotemporal FT ef-

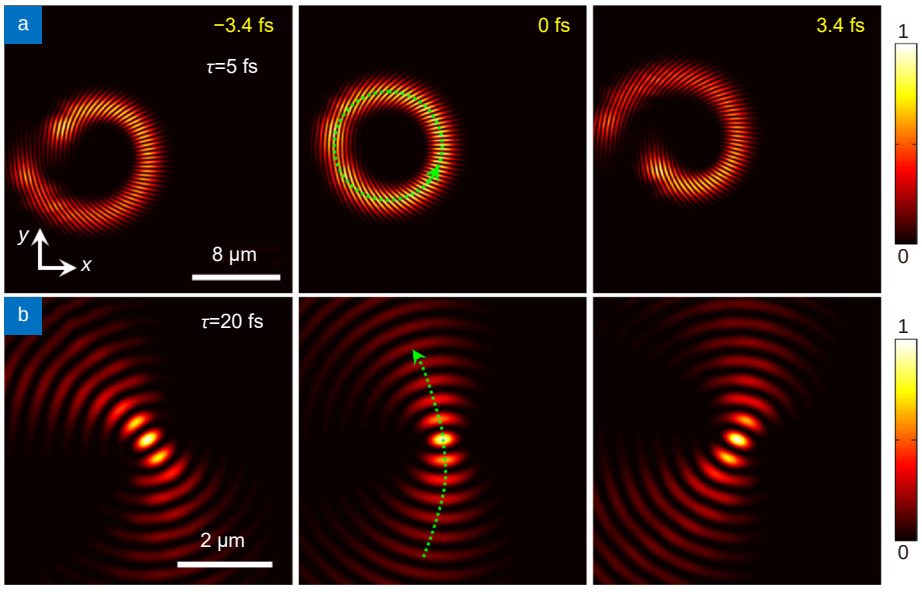

Fig. S3 | The dependence of the spatiotemporal FT effects on the pulse duration τ in the case of angular dispersion (θ =10°). (**a**) R =40 μm, α=180°, τ =5 fs. (**b**) The same as (a) except τ =20 fs. The green arrow indicates the direction of propagation path of the SPP pulses at the elapsed time given in the top right corner.

fect of the SPP pulse is also affected by the pulse duration of the incident light source.

Therefore, the propagation path of the SPP pulse and its spatiotemporal FT effect can be flexibly modulated by changing these parameters, which provides new ideas for the application of on-chip optical pulse spatiotemporal modulation, beam steering, and photon information processing.

Section 4: Supplementary movies

Supplementary Movie 1 to Movie 3 show the ultrafast evolution of the SPP pulse in the focal region subject to different dispersion corresponding to Fig. 2(e, h, k), respectively. Movie 1:θ = 0°; Movie 2: θ = 5°; Movie 3: θ = 10°.

Supplementary Movie 4 to Movie 7 show the ultrafast evolving of the SPP-Airy pulse in the focal region subject to non-dispersion (Movie 4 and Movie 5) and dispersion (Movie 6 and Movie 7) corresponding to Fig. 3(c–f), respectively. (Movie 4 and 6) present analytical results and (Movie 5 and Movie 7) present 3D-FDTD simulation results.

Section 5: Spatiotemporal FT characteristics of self-splitting SPP pulses

Here, in order to generate the self-splitting effect[S1,S2] of SPP pulse, the equivalent phase (wavefront) distribution of the slit is taken as $\varphi_1 = p_1(\pi/2 - |\beta|)^3$, where p_1 is a constant parameter that will affect the degree of self-splitting.

Figure S4(a) shows the spatial intensity distribution of the self-splitting effect of SPP pulse excited with a normal in-

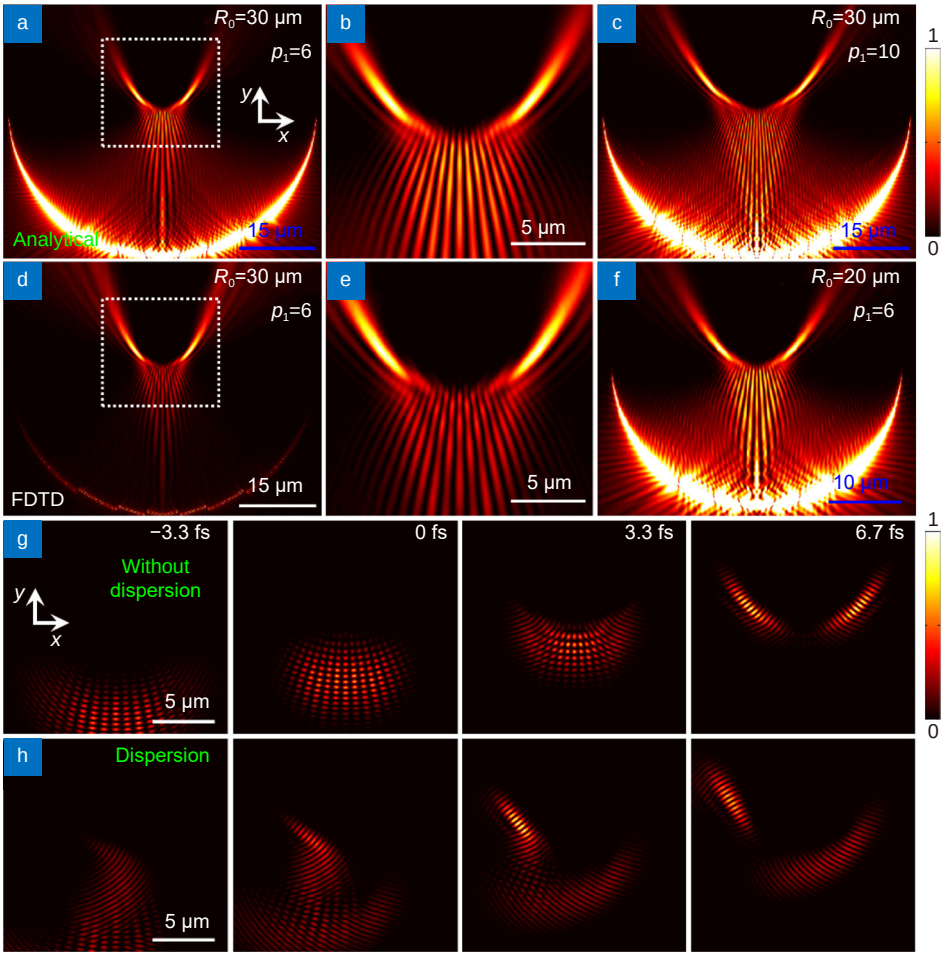

Fig. S4 | Spatiotemporal FT characteristics of self-splitting SPP pulses. (**a**) The spatial intensity distribution of the time-averaged field corresponding to the center wavelength (800 nm) in the SPP pulse without dispersion modulation. (**b**) The enlarged view of the focal area (white dashed box in (a)) , and (**g**) the timing diagram of the evolution process of the SPP pulse in the focal area under the conditions of θ =0°, R_0 =30 μm, α =180°, p_1 =6 and τ =10 fs. (**d**) and (**e**) are the FDTD simulation results corresponding to (a) and (b). (**c**) and (**f**) are similar to (a) with different parameter. (c) R_0 =30 μm, p_1 =10, (f) R_0 =20 μm, p_1 =6. (**h**) The timing diagram of the evolution process of the SPP pulse in the focal region with dispersion modulation (θ =10°). Other parameters are the same as (g). (a)-(c) and (e)-(h) are calculated results. All results are normalized by the maximum value of their focus.

cidence of a y-polarized non-dispersion femtosecond laser pulse (λ_0 = 800 nm, τ = 10 fs). The SPP pulses excited on the left and right sides of the arc slits interfere with each other to form a Bessel-Gaussian beam, which is then divided into two beams on the left and right at the focus, and propagates along a curved path (Fig. S4(b)), which is in good agreement with the FDTD simulation results under the same conditions (Fig. S4(d, e)). By comparing the SPP's field distribution with different parameters, we found that when p_1 is increased, the equivalent phase (wavefront) on the slit changes more drastically, resulting in a larger opening angle of the splitting (Fig. S4(c)). While reducing the initial radius R_0, the distance at which the beam splits is also reduced. (Figure S4(f)), meaning that we can flexibly control the degree of the splitting, as well as the location where the splitting occurs by changing these parameters.

In the time domain, under the condition of non-dispersion modulation (Fig. S4(g)), the SPP pulse in the focal area (white dashed area in Fig. S4(a)) gradually divides into two sub-pulses (t =3.3 fs) over time, and then propagate synchronously to the upper left and right (t =6.7 fs), respectively. However, when an angularly dispersed light source is used to excite the self-splitting effect, the two sub-pulses are no longer synchronized (Fig. S4(h)). This is because the dispersion modulation causes a certain time delay between the SPP sub-pulses. We found that not only the splitting time of the SPP pulse, but also the time delay of the sub-pulses can be flexibly controlled by changing the dispersion of the light source, indicating that the spatiotemporal characteristics of the self-splitting SPP pulse can be flexibly modulated by changing the structural parameters and light source's dispersion, which has great application value in the fields of on-chip ultrafast optical switching and pulse splitting.

Section 6: Spatiotemporal FT characteristics of self-focusing SPP pulses

Then, the equivalent phase (wavefront) distribution of the slit is designed as $\varphi_2 = p_2\,(\pi/2 + |\beta|)^3$ to excite the self-focusing effect[S3–S5] of SPP pulse, where p_2 is a constant parameter that will affect the degree of self-focusing.

Figure S5(a) shows the spatial intensity distribution of the excited self-focusing effect of SPP pulse with a non-dispersion femtosecond laser pulse (λ_0 =800 nm, τ =10 fs). Both the SPP pulses excited on the left and right sides of the arc slits propagate along curved paths, and then converge and interfere at the focal area to form a strong focus, which is similar to the self-acceleration and self-focusing process of the ring-shaped Airy beam in free space[S3,S4]. The FDTD simulation result (Fig. S5(d)) also reproduces the above phenomenon very well under the same conditions. The intensity distributions at different positions in the propagation direction (white dashed lines in Fig. S5(a) and S5(d)) are shown in Fig. S5(b) and S5(e), respectively. It can be seen that the intensity of the SPP in the central area is almost zero before focusing (y_1), and the energy is mainly concentrated on the left and right main lobes. While the central main lobe owns most of the energy at the focus (y_2), and eventually diverge to the surroundings (y_3). The analytical and FDTD results are in good agreement in the focal region. Subsequently, when p_2 is reduced, the self-focusing distance is also reduced (Fig. S5(c), p_2 =4). While reducing R_0, the curvature of the propagation paths of the left and right sub-beams are also reduced accordingly (Fig. S5(f)), R_0 =25 μm). Thus, the spatial propagation characteristics of the self-focusing SPP are greatly affected by these parameters.

In the time domain, under the condition of non-dispersion modulation (Fig. S5(g)), the propagation direction of the femtosecond SPP pulses excited by the left and right parts of the arc slits gradually reversed over time (for example, t = −10 fs, −6.7 fs and −3.3 fs), and then converge at the center at t =0 fs. However, when an angularly dispersed light source is used to, the propagation directions of the two sub-pulses are no longer synchronized (Fig. S5(h)), they propagate to the central area successively (t =0 fs and 3.3 fs), indicating that the time delay for the two sub-pulses to reach the focus can be flexibly modulated by changing the dispersion of the laser source, which is very similar to the principle of autocorrelator in free space. Therefore, we can flexibly modulate the position and time of the self-focusing by selecting appropriate structural parameters and light source's dispersion.

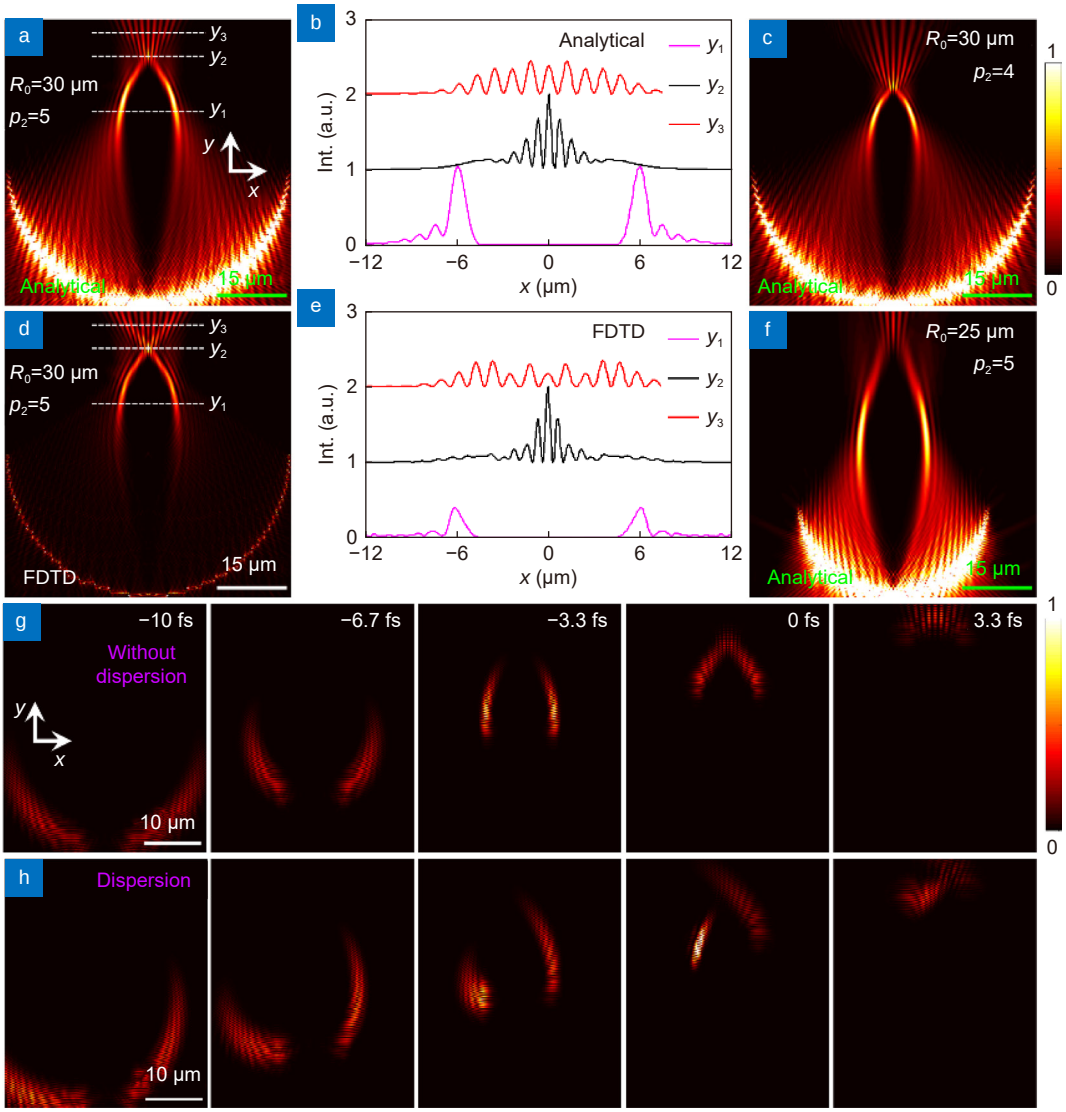

Fig. S5 | Spatiotemporal FT characteristics of self-focusing SPP pulses. The spatial intensity distribution of the time-averaged field corresponding to the center wavelength (800 nm) in the SPP pulse (**a**) without dispersion modulation, the intensity distribution at different positions in the propagation direction (white dashed lines y_1, y_2 and y_3 in (a)) (**b**), and the timing diagram of the evolution process of the SPP pulse in the focal area under the conditions of θ =0°, R_0 =30 μm, α =180°, p_2 =5 and τ =10 fs (**g**). (**d**) The FDTD simulation results corresponding to (a). (**c**) and (**f**) are similar to (a) with different parameters. (c) R_0 =30 μm, p_2 =4, (f) R_0 =20 μm, p_2 =5. (**h**) The timing diagram of the evolution process of the SPP pulse in the focal area with dispersion modulation (θ =10°). Other parameters are the same as (g). (a–c) and (e–h) are calculated results. All results are normalized by the maximum value of their focus.

References

S1. Ding CL, Koivurova M, Turunen J, Pan LZ. Temporal self-splitting of optical pulses. *Phys Rev A* **97**, 053838 (2018).

S2. Chen YH, Gu JX, Wang F, Cai YJ. Self-splitting properties of a Hermite-Gaussian correlated Schell-model beam. *Phys Rev A* **91**, 013823 (2015).

S3. Chen B, Chen CD, Peng X, Peng YL, Zhou ML et al. Propagation of sharply autofocused ring Airy Gaussian vortex beams. *Opt Express* **23**, 19288–19298 (2015).

S4. Chen XY, Zhuang JL, Li DD, Zhang LP, Peng X et al. Spatiotemporal rapidly autofocused ring Pearcey Gaussian vortex wavepackets. *J Opt* **20**, 075607 (2018).

S5. Panagiotopoulos P, Papazoglou DG, Couairon A, Tzortzakis S. Sharply autofocused ring-Airy beams transforming into non-linear intense light bullets. *Nat Commun* **4**, 2622 (2013).